JOURNAL OF CHEMICAL & ENGINEERING DATA

ARTICLE

pubs.acs.org/jced

# Comparison of Activated Carbon and Multiwalled Carbon Nanotubes for Efficient Removal of Eriochrome Cyanine R (ECR): Kinetic, Isotherm, and Thermodynamic Study of the Removal Process

M. Ghaedi,*[,†] A. Shokrollahi,[†] H. Hossainian,[†] and S. Nasiri Kokhdan[‡]

[†]Chemistry Department, Yasouj University, Yasouj 75918-74831, Iran

[‡]Young Researchers Club, Yasooj Branch, Islamic Azad University, Yasooj, Iran

**ABSTRACT:** The objective of this study was to assess the suitability and efficiency of activated carbon (AC) and multiwalled carbon nanotube (MWCNT) for the removal of Eriochrome Cyanine R (ECR) molecules from aqueous solutions. The effect of different variables in the batch method as a function of solution pH, contact time, initial dye concentration, AC and MWCNT amount, temperature, electrolyte, and so forth by the optimization method has been investigated. ECR contents were determined using a UV−vis spectrophotometer before and after ECR adsorption on the AC and MWCNT, and the removal percentage was calculated using the difference in absorbance. The sorption processes followed the pseudosecond order in addition to intraparticle diffusion kinetics models with a good correlation coefficient with the overall entire adsorption of ECR on both adsorbents. Equilibrium data fit well with the Langmuir and Tempkin models with a maximum adsorption capacity based on the Langmuir equation of (40.6 and 95.2) $mg \cdot g^{-1}$ for AC and MWCNT, respectively. Thermodynamic parameters such as change in enthalpy ($\Delta H°$) and entropy ($\Delta S°$), activation energy ($E_a$), sticking probability ($S^*$), and Gibbs free energy changes ($\Delta G°$) were also calculated. Judgment based on the obtained results of thermodynamic values shows the spontaneous and endothermic nature adsorption processes on both adsorbents.

## 1. INTRODUCTION

Most dye compounds with a complex aromatic structure, especially azo-containing ones, have a high resistance to biodegradability and are nonoxidizable by conventional biological and physical treatment. Eriochrome Cyanine R (ECR) (Figure 1) generally is completely dissolved at neutral pH in water, and the formed ionic charge species can behave as a bidentate (N, O−) univalent ligand for the chelation of several metal ions. Colored wastes present in industrial effluent are harmful to aquatic lives and environment such as rivers, lakes, and sea waters;[1,2] therefore, such wastewater prior to delivery to the environment with high efficiency must be treated. Adsorption is superior to other dye removal processes such as coagulation, oxidation, ozonation, and ultra-filtration because of its low cost, simplicity of design, and ease of operation.[3]

In this study, efficient dye removal technique species are efficiently and quantitatively transferred from the water effluent to a solid phase, and subsequently the adsorbent can be regenerated or kept in a dry place without direct contact in the environment.[4]

Most of the work is based on the adsorption behavior of activated carbon (AC)[5] and multiwalled carbon nanotubes (MWCNT)[6] due to their high adsorption capacity, which emerged from their high surface area and porous structure.

Depending on the layers involved CNTs have been referred to single-walled (SWCNTs) or MWCNTs; MWCNTs are one of the most commonly used building blocks of nanotechnology.[7] Due to their high surface area and large micropore volume CNTs are also considered to be extremely good adsorbents. Because of the unique advantage and properties of MWCNTs, they have been widely utilized for the sorption, extraction, and removal of a large number of different organic compounds.[8,9]

CNT chemical characteristics play a vital role and influence on its sorptive properties.[9,10] Therefore, the aim of the present research is based on the application of AC and MWCNT for the efficient removal of ECR, and their removal properties were compared with each other.

## 2. EXPERIMENTAL SECTION

**2.1. Materials.** All chemicals include NaOH, HCl, KCl, AC, MWCNT, and Eriochrome Cyanine R (Figure 1) with the highest purity available are purchased from Merck (Darmstadt, Germany). An accurately weighted amount of ECR was dissolved in deionized water to prepare 800 $mg \cdot L^{-1}$ as stock solution, while the working solution was prepared by daily diluting this solution. The ECR concentration evaluation was carried out using Jusco UV−visible spectrophotometer model V-570 at a wavelength of 510 nm, while the pH/ion meter model-686, thermometer Metrohm, was used for pH adjustment measurements.

**2.2. Batch Adsorption Experiments.** The influence of variables including pH, adsorbent dosage, contact time, initial dye concentration, KCl concentrations, and temperature on the adsorptive removal of ECR was investigated by batch experiments. In each experimental run onto AC and MWCNT, (100.0 and 10.0) mL of contact time of (0 to 60) min for AC and (0 to 35) min for MWCNT. ECR in (250.0 and 50.0) mL Erlenmeyer flasks was agitated with a stirrer at 350.0 rpm at a fixed control temperature. The obtained experimental data at various times, temperatures, and concentrations were fit to different models to

**Received:** April 4, 2011
**Accepted:** June 6, 2011
**Published:** June 29, 2011





dx.doi.org/10.1021/je200331u | J. Chem. Eng. Data 2011, 56, 3227–3235

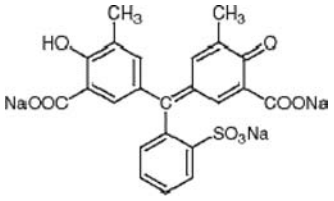


**Figure 1.** Structure of ECR.

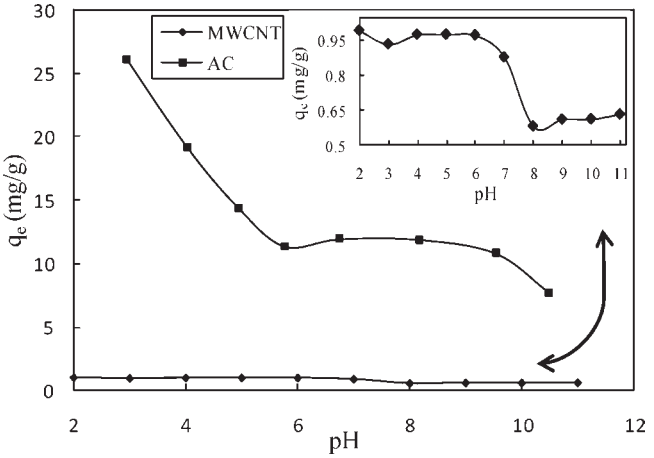


**Figure 2.** Effect of pH on the removal of ECR by (a) AC at room temperature, contact time of 45 min, adsorbent dosage of 10.0 g·L$^{-1}$, and dye concentration of 200 mg·L$^{-1}$ and (b) MWCNT at room temperature, contact time of 15 min, adsorbent dosage of 1 g·L$^{-1}$, and dye concentration of 200 mg·L$^{-1}$.

evaluate and calculate the kinetics, thermodynamics, and isotherm parameters of the adsorption process for both adsorbents at pH 3.0 and 2.0 for AC and MWCNT, respectively. The solution pH was adjusted by the addition of dilute aqueous solutions of HCl or NaOH (1.0 M and 0.1M). The removal percentage of ECR was calculated using the following relationship

$$\%\text{ECR removal} = ((C_o - C_t)/C_o)\cdot 100 \quad (1)$$

where $C_o$ (mg·L$^{-1}$) and $C_t$ (mg·L$^{-1}$) are the dye concentration at initial tim and after time $t$, respectively, and the equilibrium adsorption capacity of ECR was calculated according to the following equation:

$$q_e = (C_o - C_e)V/W \quad (2)$$

where parameters $q_e$, $C_e$, $V$, and $W$ and all respective parameters and equations in addition to respective nomenclature are presented in the end of this article.

## 3. RESULTS AND DISCUSSION

**3.1. Potentiometric Study of ECR.** According to our previous publications based on the application of the best program,[10] it was seen that ECR has four acidic groups in aqueous solution. In equilibrium, related to ECR zero, the proton level was chosen as the dicarboxylate (L) because of the very weak acidity of the salicylate −OH group, while its phenolic proton has a p$K$ more than 12. The most likely species present in the aqueous equilibrium respective to ECR are LH (log $K_1$ = 5.56), $LH_2$ (log $K_2$ = 2.85), and $LH_3$ (log $K_3$ = 2.15).

**Table 1. Comparison of the Effect of Adsorbent Dosage on the Removal of ECR at Room Temperature onto AC and MWCNT at pH 3 and 2, Respectively**

| removal (%) | | | | | | $q_e$ (mg·g$^{-1}$) | | | |
|---|---|---|---|---|---|---|---|---|---|
| AC | | | | MWCNT | | AC | | | MWCNT |
| dosage | ECR (mg·L$^{-1}$) | | | dosage | ECR | ECR (mg·L$^{-1}$) | | | ECR |
| g·L$^{-1}$ | 50 | 100 | 200 | g·L$^{-1}$ | 100 | 50 | 100 | 200 | 100 |
| 2 | 57.85 | 44.20 | 29.92 | 0.2 | 27.26 | 14.46 | 22.10 | 29.92 | 1.36 |
| 4 | 93.10 | 73.43 | 59.85 | 0.4 | 38.80 | 11.64 | 18.36 | 27.50 | 0.97 |
| 6 | 98.87 | 96.38 | 69.73 | 0.6 | 50.69 | 8.24 | 16.06 | 23.24 | 0.84 |
| 8 | 99.16 | 97.73 | 82.82 | 0.8 | 74.65 | 6.20 | 12.22 | 20.70 | 0.93 |
| 10 | | 99.73 | 91.48 | 1 | 79.19 | | 9.97 | 17.50 | 0.79 |
| 12 | | 99.45 | 92.78 | 1.2 | 88.17 | | 8.29 | 15.46 | 0.73 |
| 14 | | 99.80 | 95.34 | 1.4 | 90.04 | | 7.13 | 13.62 | 0.64 |
| 16 | | 99.67 | 95.52 | 1.6 | 92.06 | | 6.23 | 11.94 | 0.58 |
| 18 | | | 97.76 | 1.8 | 97.21 | | | 10.86 | 0.54 |
| 20 | | | 98.31 | 2 | 97.82 | | | 9.83 | 0.49 |
| | | | | 2.2 | 97.01 | | | | 0.44 |
| | | | | 2.4 | 98.54 | | | | 0.41 |
| | | | | 2.6 | 98.36 | | | | 0.38 |
| | | | | 2.8 | 99.19 | | | | 0.35 |

**3.2. Effect of pH.** Solution pH affects both aqueous chemistry and surface binding sites of the adsorbents. The effect of initial pH on the adsorption efficiency of removal of ECR at the pH range of 2.0 to 11.0 at room temperature, at an initial dye concentration of 200.0 mg·L$^{-1}$, adsorbent dosage of (10.0 and 1.0) g·L$^{-1}$ of AC and MWCNT, and contact time of 45 min and 15 min was investigated, and respective results are shown in Figure 2. It was found that the maximum percentage of ECR was obtained at pH 3 and 2 using AC and MWCNT, respectively.

The most acidic functional group of ECR easily dissociated so that the ECR molecule has net negative charges. At lower pH due to high abundance, more protons will be available, and the surface of the AC and MWCNT acquires a positive charge that leads to an increase in electrostatic attractions between the positive charge of both adsorbents in the ECR molecule that significantly improve the removal percentage.[11−13] The lower adsorption of ECR at high pH can be explained via competition of high amount of $OH^-$ ions with ECR in addition to ionic repulsion between the negatively charged surface and the anionic ECR molecules. It was seen that the most effective pH was 2 for MWCNT and 3 for AC because oxidization of MWCNT[8] lead to the generation of hydrophilic oxygen-containing groups such as carboxylic, carbonyl, lactonic, and hydroxyl groups on MWCNTs. The higher number of these functional groups on MWCNT with respect to AC results in the deprotonation of these groups at alkaline pH. Therefore, by raising their pH, the adsorption of water is more energetically favorable relative to the adsorption of ECR and the higher the adsorption on both adsorbents.[8]

**3.3. Effect of Ionic Strength.** ECR adsorption studies were carried out in the presence of potassium chloride [(0 to 4) M], and it was observed that adsorption capacities of both adsorbents for ESR are not significantly affected until a high amount of KCl which can be inferred that $Cl^-$ ions do not

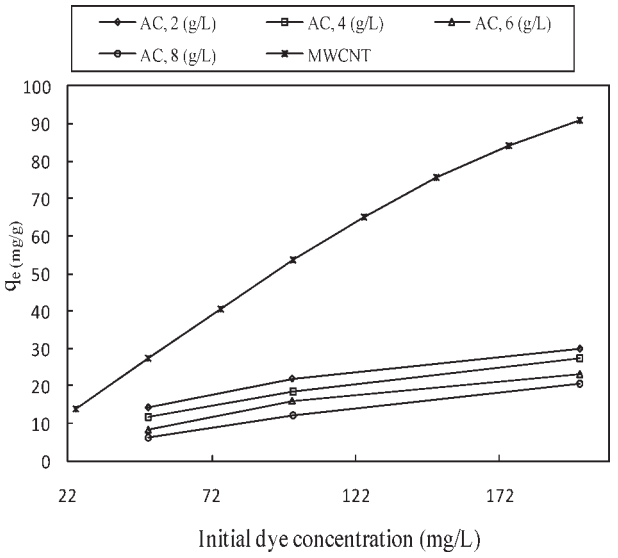


**Figure 3.** Comparison of the effect of initial dye concentration on the removal of ECR at room temperature onto a range from 2.0 to 6.0 $g \cdot L^{-1}$ of AC at pH 3 and a contact time of 41 min and also onto 1.8 $g \cdot L^{-1}$ of MWCNT at pH 2 and a contact time of 10 min.

compete with ESR functional groups. Therefore, ECR can be removed from salted water.

**3.4. Effect of Adsorbent Dosage.** The dependency of ECR adsorption to the quantity of adsorbent AC and MWCNT in the range of (2.0 to 20.0) $g \cdot L^{-1}$ and (0.2 to 2.8) $g \cdot L^{-1}$ investigated at 100.0 $mg \cdot L^{-1}$ of ECR, room temperature, and pH 3.0 and 2.0, respectively (Table 1). It was seen that, by increasing AC and MWCNT to (8.0 and 1.8) $g \cdot L^{-1}$, because of high surface area and availability of more adsorption sites, the rate of mass transfer and diffusion significantly was improved.

**3.5. Effect of Initial Dye Concentration.** The effect of the initial ECR concentration in the range of (25.0 to 200.0) $mg \cdot L^{-1}$ on the rate of sorption and quantity of amount of ESR adsorbent onto AC and MWCNT was studied in the pH of 3.0 and 2.0, respectively, using 6 $g \cdot L^{-1}$ of AC and 1.8 $g \cdot L^{-1}$ of MWCNT (Figure 3). It was seen that, by increasing the initial ESR concentration, the concentration was a driving force of mass transfer at the initial stage of adsorption on the rate of adsorption.[14]

As shown the uptake of dye is enhanced with increasing initial dye concentration. By increasing the initial dye concentration, however, the ECR removal percentage decreased, and the actual amount of adsorbed ESR per unit mass of both adsorbents significantly increased.

**3.6. Effect of Contact Time on Dye Removal.** The effect of contact time at room temperature on the sorption at 100.0 $mg \cdot L^{-1}$ of ECR is depicted in Figure 4. As can be seen using AC in the presence of AC by increasing contact time until the amount of adsorbed dye improved and further addition of contact time, the adsorption rate was not drastically increased. The initial fast rate of adsorption is attributed to ECR adsorption by the exterior surface until surface saturation of AC and finally the ESR molecule exerted onto the pores of the adsorbent particles that this phenomenon takes a relatively long contact time.[15,16] Using MWCNT as an efficient adsorbent without pore diffusion, the adsorption process reaches equilibrium very fast. As it can be seen from Figure 4, using a low amount of MWCNT as

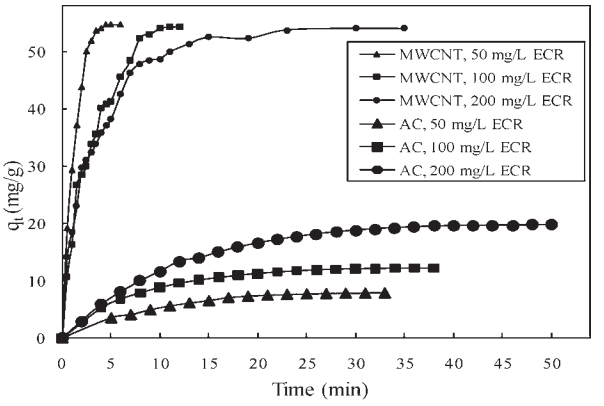


**Figure 4.** Effect of contact time on removal of (50, 100, and 200) $mg \cdot L^{-1}$ ECR onto (6, 8, and 10) $g \cdot L^{-1}$ of AC, respectively, in 100 mL volume and 1.8 $g \cdot L^{-1}$ of MWCNT in 10 mL volume, at pH 3 and 2 for AC and MWCNT, respectively, both at room temperature.

an adsorbent compared to AC leads to obtain high adsorption capacity ($q_e$).

**3.7. Effect of Temperature on Dye Removal.** To determine whether the under study adsorption process was endothermic or exothermic in nature, ESR adsorption studies were carried out at temperature in the range of (283.15 to 333.15) K, and it was seen that the rate and amount of adsorbed ESR significantly improved by raising temperature which shows the endothermic nature of the adsorption process.

The results show that the adsorption of ESR on AC and MWCNT reached a maximum value at 303.15 K for AC and 323.15 K for MWCNT. Adsorption of a solute from solution phase onto the solid−liquid interface occurs by dislodging the solvent molecule (water) from the interfacial region. Probably with rising temperature, the interaction between solvent and solid surface was reduced. Therefore, at elevated temperature due to an increase in free volume, the rate and amount of adsorption increased.

**3.8. Kinetic Parameters of Adsorption.** The kinetic parameters (helpful for determination of the rate-controlling and mass transfer step) give important information for the selective application of an efficient, low-cost, high adsorption capacity adsorbent. Thus, pseudofirst-order, pseudosecond-order,[15] Elovich,[16] and intraparticle diffusion[17] kinetic models were used for the adsorption of ECR on AC and MWCNT. The agreement between experimental data and the model-predicted values was expressed by the correlation coefficients ($R^2$, values close or equal to 1 and the relatively higher value shows the applicability of the model).

*3.8.1. Pseudofirst-Order Equation.* The Lagergren pseudofirst-order model[15] is commonly expressed in linear form as follows described by the adsorption kinetic data:

$$\log(q_e - q_t) = \log(q_e) - k_1 t/2.303 \qquad (3)$$

Generally, by plotting $\log(q_e - q_t)$ versus $t$ (linear relationship), $k_1$ and $q_e$ can be evaluated from the slope and intercept of the respective line, respectively. If the intercept is not close to $q_e$ then this means that the reaction is not likely to be first-order reaction even the obtained line and plot have a high correlation coefficient.[16]

Although the model is an application for explaining phenomena at initial stages (rapid adsorption), it cannot be applied for

**Table 2. Comparison of Adsorption Kinetic Parameters for the Adsorption of (50, 100, and 200) mg·L$^{-1}$ ECR onto (6.0, 8.0, and 10.0) g·L$^{-1}$ of AC, Respectively, at pH 3 and a Contact Time of 41 min and Also onto 1.8 g·L$^{-1}$ of MWCNT at pH 2 and a Contact Time of 10 min for Both Adsorbents at Room Temperature**

| | | | initial ECR concentration (mg·L$^{-1}$) | | | | | |
|---|---|---|---|---|---|---|---|---|
| | | | AC | | | MWCNT | | |
| model | | | 50 | 100 | 200 | 50 | 100 | 200 |
| first-order kinetic | | $k_1$ | 0.192 | 0.162 | 0.129 | 1.131 | 0.335 | 0.207 |
| | | $q_e$ (calc) | 16.92 | 16.84 | 31.17 | 73.18 | 64.46 | 39.85 |
| | | $R^2$ | 0.9673 | 0.9644 | 0.9564 | 0.9769 | 0.9216 | 0.9647 |
| second-order kinetic | | $k_2 \cdot 10^3$ | 9.963 | 10.694 | 3.591 | 13.195 | 4.924 | 8.431 |
| | | $q_e$ (calc) | 10.63 | 14.64 | 24.94 | 67.568 | 68.966 | 57.803 |
| | | $R^2$ | 0.9903 | 0.9979 | 0.992 | 0.9894 | 0.9941 | 0.9987 |
| | | $h$ | 1.13 | 2.29 | 2.23 | 60.241 | 23.419 | 28.169 |
| intraparticle diffusion | $K_{diff}$ | first regression line | 1.951 | 2.416 | 4.142 | 35.174 | 19.039 | 15.894 |
| | | second regression line | 0.412 | 0.448 | 0.602 | 3.631 | 3.117 | 2.064 |
| | $C$ | first regression line | −0.863 | 0.905 | −1.995 | −5.849 | −0.079 | 4.149 |
| | | second regression line | 5.697 | 9.602 | 15.633 | 46.384 | 43.757 | 42.971 |
| | $R^2$ | first regression line | 0.9961 | 0.9796 | 0.9846 | 0.9998 | 0.972 | 0.9788 |
| | | second regression line | 0.9414 | 0.8957 | 0.8643 | 0.7159 | 0.8973 | 0.8555 |
| Elovich | $\beta$ | | 0.393 | 0.317 | 0.179 | 0.064 | 0.067 | 0.093 |
| | α | | 2.142 | 5.035 | 4.715 | 116.2 | 52.1 | 80.4 |
| | $R^2$ | | 0.9675 | 0.9693 | 0.9766 | 0.9516 | 0.9856 | 0.9545 |
| $q_e$ (exp) | | | 7.94 | 12.15 | 19.66 | 54.65 | 54.01 | 53.76 |

the entire adsorption process. Furthermore, the calculated $q_e$ value is significantly different with experimental $q_e$ values (Table 2), which indicates that the adsorption of ECR onto AC and MWCNT do not follow a first-order reaction.

*3.8.2. Pseudosecond-Order Equation.* Because of an insufficient first-order kinetic model for the explanation of adsorption during the entire process, this necessary that fitting the experimental data be carried out using a pseudosecond-order model.[18] This model in linear form is commonly expressed as follows:

$$(t/q_t) = 1/(k_2 q_e^{\,2}) + t/q_e \quad (4)$$

It was seen that the plots of $t/q_t$ versus $t$ give a straight line that show its suitability and applicability for fitting and interpretation of experimental data. The $k_2$ and equilibrium adsorption capacity ($q_e$) values as main parameters of this model were evaluated from the intercept and slope of this line, and the respective value is presented in Table 2. The values of $R^2$ and close experimental and theoretical $q_e$ indicate that this equation produced better results than other models for the explanation of the adsorption process.

The value of initial sorption ($h$) is practically increased with the increase in initial dye concentration from (50 to 200) mg·L$^{-1}$ onto AC and MWCNT (Table 2).

*3.8.3. Elovich Kinetic Equation.* The Elovich equation[18] as another rate equation based on the adsorption capacity in linear form can be given as follows:

$$q_t = 1/\beta \ln(\alpha\beta) + 1/\beta \ln(t) \quad (5)$$

The plot of $q_t$ versus $\ln(t)$ should yield a linear relationship if the Elovich is applicable with a slope of $(1/\beta)$ and an intercept of $(1/\beta)$ $\ln(\alpha\beta)$. The Elovich constants obtained from the slope and the intercept of the straight line are reported in Table 2. The correlation coefficients $R^2$ are higher than 0.9516 showing the suitability of the model for evaluation of the adsorption process.

*3.8.4. Intraparticle Diffusion Model.* Generally, most of the dye adsorption process follows intraparticle diffusion; this model should be used to study the rate-limiting step for ECR adsorption onto AC and MWCNT. The intraparticle diffusion is commonly expressed by the following equation:

$$q_t = K_{diff} t^{1/2} + C \quad (6)$$

The values of $K_{diff}$ and $C$ were calculated from the slope and intercept of the plot of $q_t$ versus $t^{1/2}$. The $C$ value is related to the thickness of the boundary layer, and $K_{diff}$ is the intraparticle diffusion rate constant (mg·g$^{-1}$·min$^{-1/2}$); they are reported in Table 2. This plot gives two lines that the rate constant ($K_{diff}$) directly evaluated from the slope of the second regression line, while the first one represents the surface adsorption (start of adsorption) while the second one is the intraparticle diffusion.

If this plot passes through the origin, the intraparticle diffusion is the sole rate determination step ($C$ value of zero).[2] The high value of $R^2$ values (Table 2) indicate the suitability of this model and confirm that the rate-limiting step is the intraparticle diffusion process. Table 2 represents the plot between the values of intercept $C$ versus different initial dye concentrations for 6 g·L$^{-1}$ of AC and 1.8 g·L$^{-1}$ of MWCNT. The constant $C$ was found to increase for AC with increasing ECR concentration, which shows the increase of the thickness of the boundary layer and decrease of the chance of the external mass transfer. The intraparticle diffusion rate constant, $K_{diff}$, for AC and MWCNT was in the range of 0.412 to 0.602 and 2.064 to 3.631 (mg·g$^{-1}$·min$^{-1/2}$) that respective values increased for AC with increasing initial ECR concentration at fixed values (Table 2). Since the plot does not pass through the origin, the intraparticle diffusion is not the only rate-controlling step.[19]

**Table 3. Comparison of Isotherm Parameters and Correlation Coefficients Obtained from Four Linear Forms of Langmuir Models at Room Temperature for the Adsorption of Different Initial ECR Concentrations onto 6.0 g·L$^{-1}$ of AC at pH 3 and a Contact Time of 41 min and also onto 1.8 g·L$^{-1}$ of MWCNT at pH 2 and a Contact Time of 10 min**

| | $Q_m$ (mg·g$^{-1}$) | | $K_a$ (L·mg$^{-1}$) | | $R^2$ | | $R_L$ | | | |
|---|---|---|---|---|---|---|---|---|---|---|
| | | | | | | | concentration (mg·L$^{-1}$) | | | |
| | | | | | | | AC | | | MWCNT |
| Langmuir model | AC | MWCNT | AC | MWCNT | AC | MWCNT | 50 | 100 | 200 | 100 |
| Langmuir-1: $C_e/q_e = (1/K_aQ_m) + C_e/Q_m$ | 40.65 | 95.24 | 0.121 | 0.383 | 0.9999 | 0.9965 | 0.1420 | 0.0763 | 0.0397 | 0.0254 |
| Langmuir-2: $1/q_e = 1/(K_aQ_mC_e) + 1/Q_m$ | 39.68 | 86.21 | 0.126 | 0.569 | 0.9998 | 0.9929 | 0.1370 | 0.0734 | 0.0381 | 0.0173 |
| Langmuir-3: $q_e = Q_m - q_e/(K_aC_e)$ | 40.33 | 86.38 | 0.123 | 0.571 | 0.9987 | 0.9481 | 0.1400 | 0.0753 | 0.0391 | 0.0172 |
| Langmuir-4: $q_e/C_e = K_aQ_m - K_aq_e$ | 40.37 | 88.03 | 0.123 | 0.541 | 0.9987 | 0.9481 | 0.1402 | 0.0754 | 0.0392 | 0.0181 |

*3.8.5. Boyd Model Distinguishing between Film Diffusion and Particle Diffusion.* The slowest adsorption step was distinguished using the Boyd equation according to the following equation:

$$Bt = -0.4977 - \ln(1 - F) \quad (7)$$

$$\text{where } F = q_t/q_e \text{ and } B = (\pi^2 D_i)/r_0^2 = \text{time constant} \quad (8)$$

If the plot of $[-0.4977 - \ln(1 - F)]$ against $t$ (min) is linear and passes through the origin, the rate-controlling step of adsorption is the internal diffusion. It was observed that the plot is linear and Boyd intercept was near to zero which conforms to the fact that the adsorption process is controlled by intraparticle diffusion.

**3.9. Sorption Isotherms and Equilibrium.** It is possible to depict the equilibrium adsorption isotherms by plotting the solid phase concentration ($q_{eq}$; mg·g$^{-1}$) against the liquid phase concentration ($C_{eq}$; mg·L$^{-1}$) of solute to understand the adsorption capacity of adsorbent. Therefore, the Langmuir, Freundlich, Tempkin, Dubinin and Radushkevich (D-R), and Harkins−Jura (H-J) isotherm equations analyzed experimental data for the adsorption of ECR on AC and MWCNT.[2,20]

*3.9.1. Langmuir Isotherm.* The Langmuir isotherm model give information about the maximum adsorption capacity (corresponding to complete monolayer coverage) of each adsorbent which is based on equations presented in Table 3.

The correlation coefficients for all Langmuir models (Tables 3 and 4) showed strong positive evidence on the tendency of ECR adsorption onto AC and MWCNT to follow the Langmuir-1 isotherm that probably shows the homogeneous distribution of active sites of AC and MWCNT surface, since the Langmuir equation assumes that the surface is homogeneous.

The maximum monolayer capacity $Q_m$ obtained from Langmuir model was 40.6 mg·g$^{-1}$ for AC and 95.2 mg·g$^{-1}$ for MWCNT.

Essential features of the Langmuir isotherm can be expressed in terms of dimensionless equilibrium parameter $R_L$ (separation factor), which is calculated using the following equation:

$$R_L = 1/(1 + K_aC_0) \quad (9)$$

Values of $R_L$ indicate the shapes of isotherms to be either unfavorable ($R_L > 1$), linear ($R_L = 1$), favorable ($0 < R_L < 1$), and irreversible adsorption ($R_L = 0$).[21]

**Table 4. Comparison of Isotherm Parameters and Correlation Coefficients Calculated by Various Adsorption Models at Room Temperature at Different Initial ECR Concentrations onto 6.0 g·L$^{-1}$ of AC at pH 3 and a Contact Time of 41 min and also onto 1.8 g·L$^{-1}$ of MWCNT at pH 2 and a Contact Time of 10 min**

| isotherm equation | parameters | | AC | MWCNT |
|---|---|---|---|---|
| Langmuir-1: $C_e/q_e = (1/K_aQ_m) + C_e/Q_m$ | $Q_m$ (mg·g$^{-1}$) | | 40.65 | 95.24 |
| | $K_a$ (L·mg$^{-1}$) | | 0.121 | 0.383 |
| | $R^2$ | | 0.9999 | 0.9965 |
| | $X^2 = \Sigma[(q_{e,exp} - q_{e,calc})^2/q_{e,exp}]$ | from $i = 1$ to $i = m$ | 0.0026 | 3.4600 |
| Freundlich: $\ln q_e = \ln K_F + (1/n) \ln C_e$ | $1/n$ | | 0.537 | 0.372 |
| | $K_F$ (L·mg$^{-1}$) | | 5.843 | 27.963 |
| | $R^2$ | | 0.9840 | 0.9288 |
| | $X^2 = \Sigma[(q_{e,exp} - q_{e,calc})^2/q_{e,exp}]$ | from $i = 1$ to $i = m$ | 0.2060 | 8.4060 |
| Tempkin: $q_e = B_1 \ln K_T + B_1 \ln C_e$ | $B_1$ | | 9.039 | 16.401 |
| | $K_T$ (L·mg$^{-1}$) | | 1.160 | 7.076 |
| | $R^2$ | | 0.9970 | 0.9987 |
| | $X^2 = \Sigma[(q_{e,exp} - q_{e,calc})^2/q_{e,exp}]$ | from $i = 1$ to $i = m$ | 0.0534 | 0.1590 |
| Dubinin and Radushkevich (D-R): $\ln q_e = \ln Q_m - K\varepsilon^2$, $\varepsilon = RT \ln(1 + 1/C_e)$ | $Q_m$ (mg·g$^{-1}$) | | 24.67 | 67.92 |
| | $K$ ($\cdot 10^6$) | | 1.000 | 0.100 |
| | $E$ (kJ·mol$^{-1}$) = $1/(2K)^{1/2}$ | | 0.707 | 2.236 |
| | $R^2$ | | 0.8870 | 0.8837 |
| | $X^2 = \Sigma[(q_{e,exp} - q_{e,calc})^2/q_{e,exp}]$ | from $i = 1$ to $i = m$ | 2.5020 | 34.0390 |
| Harkins−Jura (H-J): $1/q_e^2 = (B_2/A) - (1/A) \log C_e$ | $A$ | | 75.758 | 526.316 |
| | $B_2$ | | 1.318 | 1.158 |
| | $R^2$ | | 0.8180 | 0.5755 |
| | $X^2 = \Sigma[(q_{e,exp} - q_{e,calc})^2/q_{e,exp}]$ | from $i = 1$ to $i = m$ | 2.9020 | 43.4020 |

| | | dye concentration (mg·L$^{-1}$) | | | | | | | |
|---|---|---|---|---|---|---|---|---|---|
| | adsorbent | 25 | 50 | 75 | 100 | 125 | 150 | 175 | 200 |
| $R_L$ | AC | | 0.142 | | 0.076 | | | | 0.0397 |
| | MWCNT | 0.0945 | 0.0496 | 0.0336 | 0.0254 | 0.0204 | 0.0171 | 0.0147 | 0.0129 |


dx.doi.org/10.1021/je200331u |J. Chem. Eng. Data 2011, 56, 3227–3235

**Table 5. Comparison of Thermodynamic Parameters for Adsorption of (50, 100, and 200) mg·L$^{-1}$ ECR onto (6.0, 8.0, and 10.0) g·L$^{-1}$ of AC, Respectively, at pH 3 and a Contact Time of 41 min and also onto 1.8 g·L$^{-1}$ of MWCNT at pH 2 and a Contact Time of 10 min**

| adsorbent | $C_0$ mg·L$^{-1}$ | parameter | T (K) 283.15 | 293.15 | 303.15 | 308.15 | 313.15 | 318.15 | 323.15 | 333.15 |
|---|---|---|---|---|---|---|---|---|---|---|
| AC | 50 | $k_c$ | 0.837 | 3.996 | 9.263 | 7.604 | 12.252 | 11.533 | 15.581 | 17.023 |
| | 100 | | 0.635 | 1.63 | 7.972 | 8.528 | 7.092 | 9.719 | 10.449 | 20.223 |
| | 200 | | 0.206 | 0.667 | 4.546 | 6.885 | 1.402 | 1.892 | 6.898 | 13.191 |
| MWCNT | 50 | $k_c$ | 0.843 | 1.243 | 2.325 | | 3.098 | | 3.447 | 29.304 |
| | 100 | | 1.125 | 1.612 | 2.644 | | 3.749 | | 9.397 | 8.963 |
| | 200 | | 1.26 | 2.131 | 3.072 | | 5.238 | | 9.999 | 18.351 |
| AC | 50 | $\Delta G^0$ (kJ·mol$^{-1}$) | 0.42 | −3.376 | −5.61 | −5.197 | −6.524 | −6.468 | −7.378 | −7.851 |
| | 100 | | 1.068 | −1.191 | −5.232 | −5.491 | −5.1 | −6.015 | −6.304 | −8.328 |
| | 200 | | 3.711 | 0.988 | −3.816 | −4.943 | −0.88 | −1.686 | −5.188 | −7.145 |
| MWCNT | 50 | | 0.401 | −0.529 | −2.127 | | −2.944 | | −3.325 | −9.356 |
| | 100 | | −0.277 | −1.163 | −2.451 | | −3.44 | | −6.019 | −6.074 |
| | 200 | | −0.544 | −1.844 | −2.828 | | −4.311 | | −6.186 | −8.059 |

| adsorbent | $C_0$ mg·L$^{-1}$ | $\Delta S^0$ J·mol$^{-1}$·K$^{-1}$ | $\Delta H^0$ kJ·mol$^{-1}$ | $E_a$ kJ·mol$^{-1}$ | $S^*$ |
|---|---|---|---|---|---|
| AC | 50 | 159.67 | 44.151 | 41.936 | $1.735 \cdot 10^{-9}$ |
| | 100 | 181.212 | 51.491 | 49.053 | $1.061 \cdot 10^{-10}$ |
| | 200 | 189.459 | 56.249 | 51.105 | $8.606 \cdot 10^{-11}$ |
| MWCNT | 50 | 160.843 | 46.587 | 39.484 | $2.803 \cdot 10^{-08}$ |
| | 100 | 126.922 | 35.874 | 30.273 | $9.651 \cdot 10^{-07}$ |
| | 200 | 147.241 | 41.411 | 36.257 | $7.262 \cdot 10^{-08}$ |

**Table 6. Comparison of $\Delta H°$ and $T\Delta S°$ in Thermodynamic Parameters for the Adsorption of (50, 100, and 200) mg·L$^{-1}$ ECR onto (6.0, 8.0, and 10.0) g·L$^{-1}$ of AC, Respectively, at pH 3 and a Contact Time of 41 min and also onto 1.8 g·L$^{-1}$ of MWCNT at pH 2 and a Contact Time of 10 min**

| adsorbent | $C_0$ mg·L$^{-1}$ | $\Delta H^0$ kJ·mol$^{-1}$ | parameter | T (K) 283.15 | 293.15 | 303.15 | 308.15 | 313.15 | 318.15 | 323.15 | 333.15 |
|---|---|---|---|---|---|---|---|---|---|---|---|
| AC | 50 | 44.151 | $T\Delta S^0$ (kJ·mol$^{-1}$·K$^{-1}$) | 45.211 | 46.807 | 48.404 | 49.202 | 50.001 | 50.799 | 51.597 | 53.194 |
| | 100 | 51.491 | | 51.31 | 53.122 | 54.934 | 55.84 | 56.747 | 57.653 | 58.559 | 60.371 |
| | 200 | 56.249 | | 53.645 | 55.54 | 57.435 | 58.382 | 59.329 | 60.277 | 61.224 | 63.118 |
| MWCNT | 50 | 46.587 | | 45.543 | 47.151 | 48.759 | - | 50.368 | - | 51.976 | 53.584 |
| | 100 | 35.874 | | 35.938 | 37.207 | 38.476 | - | 39.745 | - | 41.015 | 42.284 |
| | 200 | 41.411 | | 41.691 | 43.164 | 44.636 | - | 46.109 | - | 47.581 | 49.053 |

Considering evaluated $R_L$ values calculated at different initial ECR concentrations, it seems that the system of ECR adsorption on AC ($0.04 < R_L < 0.14$ for AC and MWCNT $0.013 < R_L < 0.095$ for MWCNT) is favorable, since the calculated $R_L$ values are very close to a lower acceptable range.

*3.9.2. Freundlich Isotherm.* The Freundlich isotherm model (multilayer adsorption) on a heterogeneous surface with a nonuniform distribution of sorption heat can be expressed in linearly according to the equation presented in Table 4.[22]

The value of $n$ depending on the heterogeneity of the adsorbent and for a favorable adsorption process should be less in the range of 1 to 10 as $1/n$ gets closer to zero.[21] The values of $K_f$ and $1/n$ were determined from the intercept and slope of linear plot of ln $q_e$ versus ln $C_e$, respectively (Table 4).

*3.9.3. Tempkin Isotherm.* The Tempkin and Pyzhev[23] model, based on decreasing adsorption heat via respective interaction between them in linear form, is represented by the equation presented in Table 4.

Values of $B_1$ and $K_T$ were calculated from the plot of $q_e$ against ln $C_e$ (Table 4). As shown in Table 4 for the Tempkin isotherm, $R^2 > 0.9970$, which is near the value of Langmuir and shows that there is a strong interaction between adsorbate molecules and adsorbent surface.

*3.9.4. Dubinin—Radushkevich (D—R) Isotherm.* The D-R model[24] provides some knowledge about the adsorbent porosity apparent free energy, and the characteristics of adsorption[24,25] are represented according to a linear equation (Table 4).

The slope of the plot of ln $q_e$ versus $\varepsilon^2$ gives $K$ (mol$^2$·kJ$^{-2}$), and the intercept yields the adsorption capacity, $Q_m$ (mg·g$^{-1}$).

The mean free energy of adsorption ($E$) can be calculated from the $K$ value using the following relationship:[26]

$$E = 1/(2K)^{1/2} \quad (10)$$

If the $E$ value lies between (8 and 16) kJ·mol$^{-1}$, the adsorption process takes place chemically, while if $E$ is less than 8 kJ·mol$^{-1}$, the adsorption process proceeds physically. In this work the $E$ value was 0.71 and 2.24 (kJ·mol$^{-1}$) for AC and MWCNT, respectively (Table 4). In this case, the D-R equation represents a poor fit of experimental data (Table 4), while the maximum capacity ($Q_m$) obtained using the D-R isotherm is (24.7 and 67.9) mg·g$^{-1}$ using AC and MWCNT adsorbent, respectively, which is significantly lower (half) than the obtained value from the Langmuir-1 model [(40.6 and 95.2) mg·g$^{-1}$] (Table 4).

*3.9.5. Harkins–Jura Adsorption Isotherm.* The Harkins–Jura adsorption isotherm[20] predicts the behavior of multilayer adsorption of adsorbate on a heterogeneous pore distribution is expressed in linear form presented in Table 4.

In this model, afterplotting $1/q_e^2$ versus log $C_e$, the respective isotherm constants and correlation coefficients were calculated and are summarized in Table 4.

Finally the correlation coefficients reported in Table 4 showed strong positive evidence on the adsorption of ECR onto AC and MWCNT which follows the Langmuir and Tempkin isotherms.

*3.9.6. Error Analysis.* In this study the equivalent mathematical statement of the $\chi^2$ test[20] is expressed as the following equation;

$$X^2 = \sum[(q_{e,exp} - q_{e,calc})^2/q_{e,exp}] \text{ from } i = 1 \text{ to } i = m \quad (11)$$

A good fit and agreement of experimental and isotherm model means the $X^2$ value will be low, meaning that this phenomenon was evaluated by carrying out by the $\chi^2$ test, By comparing the values of $X^2$ for different isotherms (Table 4) for the adsorption of ECR onto AC, it was found that the Langmuir and Tempkin models are the best models for the interpretation of ECR adsorption on both adsorbents.

**3.10. Thermodynamic Study.** Thermodynamic parameters that are required to confirm the adsorption nature of the present study can be obtained from the following equations:

$$\Delta G^\circ = -RT \ln K_c \quad (12)$$

Values of $K_c$ may be calculated from the relation $K_c = (q_e/C_e)$ at different temperatures and extrapolating to zero. The thermodynamic parameters are listed in Table 5 and 6. The negative $\Delta G^\circ$ values confirm the spontaneous nature and feasibility of the adsorption process, and decreasing its negative value while raising temperature from (283 to 333) K shows that adsorption becomes more favorable at higher temperatures. As it can be seen from Table 6, raising the temperature leads to the fact that the $T\Delta S^\circ$ phrase is prominent ($|\Delta H^\circ| < |T\Delta S^\circ|$), showing that the adsorption process is dominated by entropic rather than enthalpy changes.[18]

The values of enthalpy change ($\Delta H^\circ$) and entropy change ($\Delta S^\circ$) can be determined from the slope and intercept of plots of ln $K_c$ versus $1/T$ in the van't Hoff equation[27] as follows;

$$\ln K_c = \Delta S^\circ/R - \Delta H^\circ/RT \quad (13)$$

Also $\Delta G^\circ$ can be obtained from $\Delta H^\circ$ and $\Delta S^\circ$ evaluated from the van't Hoff equation at each temperature by means of the following equation;

$$\Delta G^\circ = \Delta H^\circ - T\Delta S^\circ \quad (14)$$

It also confirms the increased randomness at the solid–liquid interface during adsorption that shows the physical nature of adsorption at this point, asserting that physical adsorption is the predominant mechanism; the values of activation energy ($E_a$) and sticking probability ($S^*$) were estimated from the experimental data based on the modified Arrhenius equation related to surface coverage ($\theta$)[20] as the linear form.

The sticking probability ($S^*$) shows the adsorption of target analytes on adsorbent, so that the value of $0 < S^* < 1$ is dependent to temperature, while the surface coverage ($\theta$) was generally determined and evaluated from the following equation:

$$\theta = [1 - C_e/C_o] \quad (15)$$

The activation energy value estimated from the slope and intercept of plot of $\ln(1 - \theta)$ versus $1/T$ was found be at (50, 100, and 200) mg·L$^{-1}$ of ECR concentration (41.9, 49.1, and 51.1) kJ·mol$^{-1}$ on AC and (39.5, 30.3, and 36.3) mg·L$^{-1}$ on MWCNT where these positive values indicate the endothermic nature of the adsorption process. Table 5 indicates that the probability of ECR to stick on AC surface is very high as $S^* \ll 1$, which confirms that the sorption process follows physisorption through hydrogen bonding or van der Waals forces.

## 4. CONCLUSION

The results of this work can be summarized as follows: (i) AC and MWCNT are two promising adsorbents for ECR removal from wastewater. A small amount (6, 8, and 10 g·L$^{-1}$) of AC could almost remove over (98.9, 97.7, and 91.5) % of (50, 100, and 200) mg·L$^{-1}$ of ECR at the range of (20 to 36) min of contact time, and 1.8 g·L$^{-1}$ of MWCNT could remove over 97.2 % of 100 mg·L$^{-1}$ of ECR at a time of 10 min. (ii) The solution pH has important bearing on the extent of adsorption of the dye on AC and MWCNT, which indicates that the pH is more important in the controlling of adsorption rather than the nature of the surface sites. (iii) The kinetic study of ECR on AC and MWCNT was investigated using pseudofirst-order, pseudosecond-order, Elovich, and intraparticle diffusion equations. It was seen that ECR adsorption on AC follows the pseudosecond-order and Elovich with intraparticle diffusion models, while the process on MWCNT follows the pseudo-second-order and Elovich models. (iv) The experimental data for both adsorbents showed a good fit to the Langmuir-1 isotherm, additionally, and those obtained have good agreement with Tempkin model, while the data did not agree with Freundlich, Harkins–Jura (H-J), and Dubinin and Radushkevich (D-R) isotherm models. (vi) MWCNT in comparison with AC has a higher adsorption capacity per 1.0 g of MWCNT (mg·g$^{-1}$), while it reaches equilibrium at shorter time. (vii) Physical forces as well as ionic interaction are responsible for the binding of ECR with AC. This work confirms that the AC and MWCNT could be used for the removal of ECR dye from wastewater.

## AUTHOR INFORMATION

**Corresponding Author**
*E-mail: m_ghaedi@mail.yu.ac.ir.

## NOMENCLATURE

| | |
|---|---|
| $C_o$ | initial dye concentration (mg·L$^{-1}$) |
| $t$ | time (min) |
| $C_t$ | dye concentration (mg·L$^{-1}$) at time t |
| $q_e$ | equilibrium adsorption capacity (mg·g$^{-1}$) |

$C_e$ dye concentration ($mg \cdot L^{-1}$) at equilibrium
$V$ volume of solution (L)
$W$ weight of adsorbent (g)
$k_1$ rate constant of pseudofirst order adsorption ($min^{-1}$)
$k_2$ second-order rate constant of adsorption ($g \cdot mg^{-1} \cdot min^{-1}$)
$h$ second-order rate constants ($mg \cdot g^{-1} \cdot min^{-1}$)
$\alpha$ initial adsorption rate ($mg \cdot g^{-1} \cdot min^{-1}$)
$\beta$ desorption constant ($g \cdot mg^{-1}$)
$C$ intercept of intraparticle diffusion (related to the thickness of the boundary layer)
$K_{dif}$ rate constant of intraparticle diffusion ($mg \cdot g^{-1} \cdot min^{-1/2}$)
$F$ fraction of solute adsorbed at any time $t$ ($mg \cdot g^{-1}$)
$D_i$ effective diffusion coefficient of adsorbate in adsorbent phase
$r_o$ radius of adsorbent particles (m)
$Q_m$ maximum adsorption capacity reflected a complete monolayer ($mg \cdot g^{-1}$) in Langmuir isotherm model
$K_a$ Langmuir constant or adsorption equilibrium constant ($L \cdot mg^{-1}$) that is related to the apparent energy of sorption
$R_L$ Dimensionless equilibrium parameter (separation factor)
$K_F$ isotherm constant indicate the capacity parameter ($mg \cdot g^{-1}$) related to the intensity of the adsorption
$n$ isotherm constant indicate the empirical parameter ($g \cdot L^{-1}$) related to the intensity of the adsorption
$T$ absolute temperature in kelvin
$R$ universal gas constant ($8.314\ J \cdot K^{-1} \cdot mol^{-1}$)
$B_1$ related to the heat of adsorption ($B_1 = RT/b$)
$b_T$ constant related to the heat of adsorption
$K_T$ equilibrium binding constant
$K$ constant related to the adsorption energy at the D-R isotherm ($mol^2 \cdot kJ^{-2}$)
$Q_m$ theoretical saturation capacity at the D-R isotherm
$\varepsilon$ Polanyi potential at the D-R isotherm
$E$ mean free energy of adsorption
$B_2$ isotherm constants in the Harkins−Jura adsorption isotherm
$A$ isotherm constants in the Harkins−Jura adsorption isotherm
$X^2$ chi-squared test statistic
$q_{e,exp}$ experimental data of the equilibrium capacity ($mg \cdot g^{-1}$)
$q_{e,calc}$ equilibrium capacity obtained by calculating from the isotherm model ($mg \cdot g^{-1}$)
$\Delta G°$ free energy change ($kJ \cdot mol^{-1}$)
$\Delta H°$ heat of adsorption ($kJ \cdot mol^{-1}$)
$\Delta S°$ standard entropy ($kJ \cdot mol^{-1} \cdot K^{-1}$)
$K_c$ thermodynamic equilibrium constant
$E_a$ activation energy of adsorption ($kJ \cdot mol^{-1}$)
$S^*$ sticking probability indicates the measure of the potential of an adsorbate to remain on the adsorbent indefinite
$\theta$ surface coverage
$R^2$ correlation coefficient

## REFERENCES


(1) Greene, J. C.; Baughman, G. L. Effects of 46 dyes on population growth of fresh green algae Selenastrum capricornutum. *Text. Chem. Color* **1996**, *28*, 23.

(2) Khaled, A.; El Nemr, A.; El-Sikaily, A.; Abdelwahab, O. Removal of Direct N Blue-106 from artificial textile dye effluent using activated carbon from orange peel: Adsorption isotherm and kinetic studies. *J. Hazard. Mater.* **2009**, *165*, 100–110.

(3) de Lima, R. O. A.; Bazo, A. P.; Salvadori, D. M. F.; Rech, C. M.; Oliveira, D. P.; Umbuzeiro, G. A. Mutagenic and carcinogenic potential of a textile azo dye processing plant effluent that impacts a drinking water source. *Mutat. Res.* **2007**, *626*, 53–60.

(4) Ghaedi, M.; Shokrollahi, A.; Kianfar, A. H.; Mirsadeghi, A. S.; Pourfarokhi, A.; Soylak, M. The determination of some heavy metals in food samples by flame atomic absorption spectrometry after their separation-preconcentration on bis salicyl aldehyde, 1,3 propan diimine (BSPDI) loaded on activated carbon. *J. Hazard. Mater.* **2008**, *154*, 128–134.

(5) Ghaedi, M.; Shokrollahi, A.; Kianfar, A. H.; Pourfarokhi, A.; Khanjari, N.; Mirsadeghi, A. S.; Soylak, M. Preconcentration and separation of trace amount of heavy metal ions on bis(2-hydroxy acetophenone)ethylendiimine loaded on activated carbon. *J. Hazard. Mater.* **2009**, *162*, 1408–1414.

(6) Chen, G. C.; Shan, X. Q.; Zhou, Y. Q.; Shen, X. E.; Huang, H. L.; Khan, S. U. Multiwalled Carbon Nanotubes as Adsorbents for the Kinetic and Equilibrium Study of the Removal of Alizarin Red S and Morin. *J. Chem. Eng. Data* **2011**, *169*, 912.

(7) Tuzen, M.; Saygi, K. O.; Soylak, M. Solid phase extraction of heavy metal ions in environmental samples on multiwalled carbon nanotubes. *J. Hazard. Mater.* **2008**, *152*, 632–639.

(8) Tuzen, M.; Soylak, M. Multiwalled carbon nanotubes for speciation of chromium in environmental samples. *J. Hazard. Mater.* **2007**, *147*, 219–225.

(9) Xie, X.; Gao, L.; Sun, J. Thermodynamic study on aniline adsorption on chemical modified multi-walled carbon nanotubes. *Colloids Surf., A* **2007**, *308*, 54–59.

(10) Shokrollahi, A.; Ghaedi, M.; Niband, M. S.; Rajabi, H. R. Selective and sensitive spectrophotometric method for determination of sub-micro-molar amounts of aluminium ion. *J. Hazard. Mater.* **2008**, *151*, 642–648.

(11) Shokrollahi, A.; Ghaedi, M.; Ghaedi, H. Potentiometric and spectrophotometric studies of copper(II) complexes of some ligands in aqueous and nonaqueous solution. *J. Chin. Chem. Soc.* **2007**, *54*, 933–940.

(12) Ghaedi, M.; Hassanzadeh, A.; Nasiri Kokhdan, S. Multiwalled Carbon Nanotubes as Adsorbents for the Kinetic and Equilibrium Study of the Removal of Alizarin Red S and Morin. *J. Chem. Eng. Data* **2011**, *56*, 2511–2520.

(13) Duran, A.; Tuzen, M.; Soylak, M. Preconcentration of some trace elements via using multiwalled carbon nanotubes as solid phase extraction adsorbent. *J. Hazard. Mater.* **2009**, *169*, 466–471.

(14) Tuzen, M.; Saygi, K. O.; Usta, C.; Soylak, M. Pseudomonas aeruginosa immobilized multiwalled carbon nanotubes as biosorbent for heavy metal ions. *Biol. Technol.* **2008**, *99*, 1563–1570.

(15) Acharya, J.; Sahu, J. N.; Sahoo, B. K.; Mohanty, C. R.; Meikap, B. C. Removal of chromium(VI) from wastewater by activated carbon developed from Tamarind wood activated with zinc chloride. *Chem. Eng. J.* **2009**, *150*, 25–39.

(16) Chien, S. H.; Clayton, W. R. Application of Elovich equation to the kinetics of phosphate release and sorption on soils. *Soil Sci. Soc. Am. J.* **1980**, *44*, 265–268.

(17) McKay, G. The adsorption of dyestuff from aqueous solution using activated carbon: analytical solution for batchadsorption basedonexternal mass transfer and pore diffusion. *Chem. Eng. J.* **1983**, *27*, 187–195.

(18) Hosseini, S. J.; Nasiri Kokhdan, S.; Ghaedi, A. M.; Moosavian, S. S. Comparison of Multiwalled Carbon Nanotubes and Activated Carbon for efficient removal of methyl orange: kinetic and thermodynamic investigation. *Fresen. Environ. Bull.* **2011**, *20*, 219–234.

(19) Weber, W. J.; Morris, J. C. Kinetics of adsorption on carbon from solution. *J. Sanit. Eng. Div. Am. Soc. Civil Eng.* **1963**, *89*, 31–59.

(20) Amin, N. K. Removal of direct blue-106 dye from aqueous solution using new activated carbons developed from pomegranate peel: Adsorption equilibrium and kinetics. *J. Hazard. Mater.* **2009**, *165*, 52–62.

(21) Senturk, H. B.; Ozdes, D.; Gundogdu, A.; Duran, C.; Soylak, M. Removal of phenol from aqueous solutions by adsorption onto organomodified Tirebolu bentonite: Equilibrium, kinetic and thermodynamic study. *J. Hazard. Mater.* **2009**, *172*, 353–362.

(22) Freundlich, H. M. F. Über die adsorption in lösungen. *Z. Phys. Chem. (Leipzig)* **1906**, *57A*, 385–470.

(23) Tempkin, M. J.; Pyzhev, V. Kinetics of ammonia synthesis on promoted iron catalysis. *Acta Physiochim. URSS* **1940**, *12*, 327–356.

(24) Dubinin, M. M. Modern state of the theory of volume filling of micropore adsorbents during adsorption of gases and steams on carbon adsorbents. *Zh. Fiz. Khim.* **1965**, *39*, 1305–1317.

(25) Radushkevich, L. V. Potential theory of sorption and structure of carbons. *Zh. Fiz. Khim.* **1949**, *23*, 1410–1420.

(26) Panda, G. C.; Das, S. K.; Guha, A. K. Jute stick powder as a potential biomass for the removal of congo red and rhodamine B from their aqueous solution. *J. Hazard. Mater.* **2009**, *164*, 374–379.

(27) Ghaedi, M.; Shokrollahi, A.; Tavallali, H.; Shojaiepoor, F.; Keshavarz, B.; Hossainian, H.; Soylak, M.; Purkait, M. K. Activated carbon and multiwalled carbon nanotubes as efficient adsorbents for removal of arsenazo(III) and methyl red from waste water. *Toxicol. Environ. Chem.* **2010**, *93*, 438–449.